CHEMICAL PHYSICS AND BIOLOGY

This very large chapter includes Soft Matter, and more precisely Polymers, and Biological Macromolecules. The latter part originates in previous studies of the structure and dynamics of water. It was realized some years ago that water has especially interesting properties when located in the vicinity of a hydrophilic or a hydrophobic surface. This led to a combined study of structural and dynamical properties of Proteins and of the water that is associated to them. It is interesting to note that a similar evolution occurred in Polymer Physics. There is a growing interest for water-soluble macromolecules, and/ or for copolymers with water-soluble sequences. This leads to conformations that are different from the structures that are usually considered. In some cases, the polymers are biological molecules that are studied in conditions very different from their normal working ones. Thus, there is a significant overlap between these apparently different topics. Among others, there is an interest in showing the strong similarity between the structure of a denaturated biological molecule and that of a synthetic polymer. Work in the second area focused on amorphous and mesomorphous Polymers in the bulk and at interfaces, on Gels, and on Polyelectrolytes. The first part was interested in the static and dynamic properties of soluble and membrane proteins and their associated water. It is indeed accepted that hydration water plays a central role in the stability and function of biological macromolecules. Therefore, it is important to look for the relation between structure, dynamics, and hydration water in proteins.
The neutron scattering experiments were performed essentially with the small angle spectrometers for the structures, by time-of-flight and spin-echo inelastic scattering techniques for the dynamics, and by reflectometry for interfaces.

1. BIOLOGY

1.1. Dynamics of proteins.

The dynamics of a photosynthetic protein, C-phycocyanin (CPC), was studied. This comprises the dynamics of the protein itself as well as of the water that is located at its immediate vicinity. Dynamical studies of the protein as a function of temperature and of the rate of hydration were made by time-of-flight technique, with the Mibemol spectrometer. They led to split the hydrogen atoms into motionless and mobile fractions. As temperature is varied, a dynamical transition is found at approximately 250 K ; it corresponds to the appearance of diffusive motions inside the protein. The radius of the diffusion sphere of the hydrogen atoms in the surface residues remains constant, at approximately 2 Å as temperature changes. But the fraction of motionless atoms decreases as temperature increases and reaches a limit that corresponds to the fraction that lies on the surface.

1.2. Dynamics of water.

A complementary study of the dynamics of the hydration water, in direct contact with CPC, was performed. In order to eliminate the contribution from bulk water, this was realized on powders at hydration rates such that the proteins are functional. Samples hydrated respectively with H_2O and D_2O were used for these experiments on Mibemol. The data may be interpreted with stretched exponentials, corresponding to a distribution of relaxation times for water. The average relaxation time varies as q^{-2}, where q is the momentum transfer. This leads to a diffusion constant equal to $1.5 \times 10^{-6} cm^2/s$, smaller than the 2×10^{-5} cm^2/s of bulk water. Thus, the hydrophylic surface has a slowing down effect on hydration water.
These results were also compared with those of a "model" system, made of supercooled water in a porous Vycor silica glass with large specific surface- 116 m^2/g. The latter is made of interconnected cylindrical pores of approximately 50 Å diameter, and is very hydrophilic. Two different hydration rates for Vycor were used. The quasi-elastic incoherent scattering experiments were made as a function of temperature. The data lead to a stretched exponential function, $\exp[-(t/\tau)^{\beta}]$. The relaxation time τ varies as q^{-2}. This leads to a diffusion coefficient equal to 1.1×10^{-5} cm^2/s, again smaller than that of bulk water. The exponent β is interpreted by a distribution of relaxation times corresponding to motions inside cages with a distribution of sizes. These structural and dynamical studies show that at room temperature, interfacial water behaves as supercooled water.
The influence of water was also specified by looking at changes in the internal dynamics of two globular proteins as one goes from a hydrated powder to a solution. This was realized on lysozyme and myoglobin. It was made on the time-of-flight spectrometer IN6 at ILL. Various hydration rates in D_2O were used. It was shown that surface residues progressively get a local diffusive motion as the protein is hydrated until there is a water monolayer.

Further hydration increases the velocity of this diffusion, but does not involve more residues. Finally, the relaxation time in a solution is two times smaller than for a monolayer, with an amplitude of the motion three times larger.
Finally, the dynamics of hydrogen bonds was studied on a water/ dimethylsulfoxide (DMSO) mixture. The latter interacts strongly with water by forming H bonds. The mixture that was used (1DMSO/2H_2O) is eutectic, and is characterized by a very large decrease in the crystallization point, located at -70°C. Quasi-elastic neutron scattering experiments with deuterated DMSO allows the observation of the motion of the protons of water. They show that the dynamics is slower : the diffusion coefficient is 4 times smaller in this mixture than in pure water. A more surprising result is that the H-bond lifetime is found to be unchanged, whereas a longer time might be expected. These results indicate that hydrogen bonds are stronger than in pure water.

I.3. Structure- dynamics- function relationship

A collaboration with the Service de Biophysique des Protéines et des Membranes of CEA/Saclay was set up in order to study the relation between structure, dynamics and function of membrane proteins. Its aim is to understand completely the energetics of protein folding, and to establish a precise relationship between the structure and the functionality of these macromolecules. To this end, it is necessary to know the three dimensional structure of these proteins. It is also important to characterize with the best possible precision their internal motions. The most interesting time scales are between pico- and nanoseconds (10^{-12} to 10^{-9} s). They are accessible by inelastic neutron scattering. This work is done with membrane proteins involved in the first stages of photosynthetic processes in purple bacteria. Reaction Centers (RC) and light harvesting proteins (LH1 and LH2) were used. They form an interconnected protein network in the membrane, are available in large amount, and their structure is known.
Two examples are discussed in the highlights. The first one deals with time-of-flight experiments, giving access to motions with times in the picosecond range in the protein. The second one allows for a comparison of the collective motions in RC and LH2 by neutron spin-echo technique, for times about nanoseconds (10^{-9} s). An example of structure determination by Small Angle Neutron Scattering (SANS) for LH1 is also discussed. A combination of inelastic neutron scattering techniques and more classical methods in Biophysics such as absorption of light and vibrational spectroscopies makes it possible to study the relation between structure, dynamics, and functionality. This is a part of the PhD thesis of S. Dellerue.

I.4. Denaturated proteins.

A second kind of studies is intermediate between polymers and Biology. It involves denaturated proteins, and the possible similarities between their behavior and that of synthetic polymers. Denaturation was made either by heating or by using a strong denaturing agent, guanidinium chloride (GdmCl). Small-angle neutron studies of yeast phosphoglycerate kinase PGK denaturated by GdmCl show an excluded volume behavior, very similar to what was observed on neutral synthetic polymers. The second virial coefficient was measured, and is in agreement with the theoretical predictions for polymers. Similar results were obtained with beta-casein and neocarzinostatin (NCS) denaturated by GdmCl (PhD thesis of V. Receveur).
NCS denaturation by heating was studied in detail by a combination of SANS with other techniques. This protein has a structure made of a single domain, is very analogous to that of immunoglobulins, and also is present in other proteins. Three stages were observed during the denaturation. In the first one, the size remains almost constant. This is reminiscent of the "molten globule". Then, the radius increases until a reversible endothermic transition. The latter corresponds probably to the breaking of hydrogen bonds. In the last regime, the molecule reaches a final state where NCS behaves as an ideal chain, without any interactions. This corresponds to the so-called "theta" regime in polymer Physics.

2. POLYMERS.

Polymer studies are an excellence area of L.L.B. They dealt essentially with mesomorphous polymers at rest and under shear and elongation stresses, gels, and interfaces. Some experiments were also made on polyelectrolytes and on the dynamics of chains in the vicinity of the theta point.

2.1. Mesomorphous polymers.

The Liquid Crystalline Polymers (LCP) that were considered have comb-like structures, with a mesogenous part grafted on the main chain through a flexible spacer. An important effort on the synthesis allowed us to get monodisperse mass fractions. This made possible the determination by Small Angle Neutron Scattering (SANS) of the variation of the radius of gyration with molecular weight. At rest, it has the same variation as for a gaussian chain in the isotropic phase. In the nematic phase, it has an exponent intermediate between the gaussian and the random self-avoiding walk values. In the smectic phase, the chains are confined between the mesogenic layers. In the direction parallel to the layers, they have a gaussian character. In the transverse direction, the exponent implies a stretching of the polymers, therefore validating the assumption of jumps between successive layers.
Two kinds of deformations were studied.

A work under shear showed the richness of the possible behaviors by a combination of large angle and SANS observations. The former gives the orientation of the director. The latter are made in the three planes defined by the velocity, velocity gradient, and neutral vectors. For a polymer having both a nematic and a smectic phase, a transition was found : in the high temperature nematic phase, the director is parallel to the velocity. For low temperatures, it orders along the neutral axis. This is coupled to a change in the orientation of the chains: for high temperatures, they are parallel to the mesogens, while at lower temperatures, they are normal to the director. This transition may be interpreted by assuming a coupling between smectic fluctuations and shear.
A work under uniaxial extension also combined SANS, X-rays, and rheological measurements. Introducing the parameter " duration of relaxation after stopping the deformation" allowed for a study of the dynamics of a chain for various values of the diffraction vector q. In order to extract the effect of the comb architecture from that of the nematic interactions, two isomers were prepared in similar thermal conditions. The first one was in the isotropic phase. The second one was in the nematic phase. The experiments in the isotropic phase show that the chain is as flexible as the corresponding amorphous polymer. But both the dynamics and the rheology are non classical: the relaxation time and the viscosity have molecular weight dependences that are more important than for linear polystyrene for instance. Under uniaxial applied strain, the rate of deformation of a single chain is constant, but smaller than for the macroscopic sample. This might be explained by assuming the existence of clusters. The latter are related to the existence of temporary junctions between the teeth of the combs. In the nematic phase, the deformation is also pseudo-affine. But it relaxes as a stretched exponential : the nematic interactions slow down the local relaxation of the chains (PhD thesis of V. Fourmaux-Demange).

2.2. Gels.

The work on gels dealt with their structure, in the various cases discussed below, as well as other phenomena occurring in these structures, because of their interfacial and confining properties. Therefore the study of liquid mixtures in Vycor is included in this part.
Studies concerning the structures concerned complexes made by the association of polymers, and model systems describing composite materials made of polymer and mineral charges.

Associative gels

The former gels were made in water by hydrogen bonding between polyacids and polybases. They may then be controlled by changing the pH for instance. Comparing the structures of free and of complexed chains in similar conditions allowed us to show by contrast variation that complexation is stoichiometric, and that complexed chains are tightly bound together and have compact structures.
Gels may also form, as for instance in methyl-cellulose, by associating chains with hydrophylic and hydrophobic sequences. Agregation in this case was considered in the dilute regime, where gelation is not possible, and where phase separation may eventually occur and be studied. This was done as a function of temperature by SANS and by elastic and quasi-elastic light scattering. The results indicate that there is a wide distribution of masses that decreases as a power law with increasing masses. However the aggregates are not self-similar because growth and local densification occur together.

Composites

Model composite materials are made with two types of spheres, respectively made of silica and of nanolatex. The degree of aggregation is also controlled by pH. The composites were studied by SANS and by rheological measurements for various sizes and stretching. The results are currently being interpreted with a computer simulation.

Confining effects

Two applications were considered. Both show the confining effects in gels. They show its influence on a first and a second order transition. SANS allows us to follow the processes in a confining medium because it is easy to eliminate its contribution to the scattering.
The confining effect of gels in crystalline nucleation of a protein - lysozyme- was studied. It may lead either to a promoting or to an inhibiting effect.
Agarose gel is in the first class. It was shown by SANS that the gel is an inert medium for the protein, and that aggregates with sizes larger than 500 Angström are present, as in solutions. But as one lowers temperature, their number becomes larger in a gel.
Silica gels belong to the second class. It was shown that a fraction of the molecules adsorb on the inner surface of the gel. It was possible to determine by SANS the effective fractal dimension of this adsorbed layer. When the solution is under saturated, the dimension is that of the gel. By increasing oversaturation, the dimension increases and goes to a limiting value on the order of 3.4. Because of this adsorption, the concentration in the solution decreases, and this may explain the decrease of the nucleation rate. Crystal growth seems to be related to desorption.

Vycor glass was used for its confining properties to study by SANS a critical mixture of alcane and perfluoroalcane. The temperatures that were considered were both above and below the critical temperature of the mixture. The latter has the interesting property that both components have very similar wetting properties. The results seem to indicate that the latter do not play a central role. The observed signal is interpreted as the sum of an Ornstein- Zernicke contribution, and another one related to the interactions between Vycor, a superficial layer rich in one of the components and a core rich in the other one. This allowed the observation of critical fluctuations the size of which may be significantly larger than the pore size.

2.3. Polymer solutions.

Dynamics at the Theta point.

A detailed study of the dynamics of a linear chain in the vicinity of the theta temperature was made by Spin Echo. It shows that the relevant length in the semi-dilute regime is the diameter of the tube rather than the screening length. It was also shown that the local viscosity η_{loc} depends on the concentration C of the solution :
$\eta_{loc} = \eta_0 (1+BC)$, where η_0 is the solvent viscosity, and B is a constant that vanishes when the solvent becomes good.

Shearing of polymer solutions.

This is the subject of a thesis made in collaboration with ILL (PhD thesis of I. Morfin). It analysed by SANS the concentration fluctuations induced by shear, and connected them with small-angle light scattering and rheological measurements. Two regimes are found. In the first one, the fluctuations are enhanced by shear. Then, fluctuations diverge and there is a phase separation into two regions respectively rich and poor in polymers. This transition occurs either by increasing the mechanical perturbation or by lowering temperature. The latter brings the mixture at rest closer to the coexistence curve.

Polyelectrolytes.

Studies of the form factor of polyelectrolytes were extended to Sodium sulfonate polystyrene in the presence of multivalent ions, Ca^{2+} and La^{3+}. For high concentrations, trivalent ions lead to a phase separation that is attributed to interchain linking. More precisely, it is observed on the form factor that this leads to the individual collapse of the chains. The effect of Calcium ions seems to be similar, and this is more surprising because there is no phase separation in this case. But there is probably a local thickening of the chains.
We chose to select a work that is external to our group in this area. This was realized by a team of Institut Charles Sadron (Strasbourg) both at LLB and ILL and deals with polyelectrolyte star-shaped polymers (see highlights). Two peaks are observed in the scattered intensity. The first one varies as $C^{-1/3}$, and corresponds to the average distance between centers of the stars. The second one corresponds, in semi-dilute solutions, to the average screening length of the solution. In the dilute regime, it becomes the average on a star of the screening length, that decreases as one goes from the periphery of the star towards its center.

2.4. Interfaces.

Proteins and polymers at interfaces.

The work on polymers at interfaces also considered macromolecules with biological origin, namely lipase and beta casein. The first one is an enzyme with an activity that increases significantly at the oil/ water interface. Neutron reflectivity experiments show that the enzyme is adsorbed, and that the superficial layer has the size of the molecule. In the presence of an anionic surfactant, SDS, the layer does not change, thus indicating that there are few interactions between species with same charge. In the presence of a cationic surfactant, TTAB, adsorption increases. In the vicinity of the bulk precipitation point, there appears a thick layer. This seems to imply the possible formation of complexes at the surface. For both cases, when the surfactant concentration reaches the critical micellar concentration (CMC), a small amount only of the enzyme is detected at the surface. The adsorbed layer becomes dilute, and its width becomes on the order of five times that of lipase alone. A possible interpretation is in terms of unfolding of lipase.
The adsorption of a thermosensitive polymer, poly(N-isopropylacrylamide) (PNIPAM), in the presence of SDS has also been studied at the air/ water interface (PhD thesis of B. Jean). The adsorbed layer density increases with temperature, an effect due to a decrease in the solvent quality. In the presence of SDS, adsorption of PNIPAM is modified above the critical aggregation concentration (CAC). The polymer is then progressively displaced from the surface at all temperatures studied. The concentration profiles suggest the presence of micellar- surfactant complexes in the adsorbed layer (see highlights).

Beta casein is a naturally unfolded protein, which adsorbs at the air/water interface. A simplified model was studied. Assuming a symmetrical structure of hydrophilic and hydrophobic sequences, it was possible to get a phase diagram in a temperature concentration plane. The various measurable quantities as well as the structure of the protein were determined in all the regimes of this diagram.

Polymers at the surface of vesicles.

Finally, polymers were grafted on vesicles in order to study their stability and their sizes as a function of the chains and of temperature. The radius increases as one heats the system, without changing noticeably the polydispersity. The characteristic time for growth decreases as membrane concentration increases. This implies a fusion of the latter. The temperature dependence may be explained by the existence of a potential barrier related to the existence of grafted chains. Addition of macromolecules leads to the formation of micelles, and to the destruction of vesicles. It seems that large masses have smaller perturbation effects on membranes. This might correspond to an effect predicted by Lipowsky, where isolated grafted chains create a tension effect in the membrane.

Polymer-polymer interfaces.

Finally, we studied the interface between a polymer melt, where the chains are free, and a network, where they are interconnected (PhD thesis of G. Bacri). The characteristics of the network (mesh size) and of the melt (length of the chains) are controlling the width of the interface. The aim of this work is to study the extent to which a modification of the width of the interface changes its mechanical properties, and more precisely its resistance to fracture (see highlights).

3. PERSPECTIVES.

In Biology, we intend to continue the following soaring activities :

i)-Denaturated states of proteins.

We will compare denaturation in various conditions:
1) by a chemical agent, namely guanidinium chloride,
2) by heating up or cooling down,
3) by pressure, which has hardly been studied.
Both the structure and the dynamics of the native and unfolded states will be studied by neutron and X-ray scattering techniques. Circular dichroism, static and time-resolved fluorescence, Differential Scanning Calorimetry and Fourier Transform Infra-Red techniques will be associated with the previous ones.
Kinetic studies will also be made in the presence of chemical denaturating agents, in order to characterise the intermediate states during denaturation and renaturation of a protein such as NCS, that we already studied.

ii)-Structure-dynamics- function relationship

This will be considered for soluble as well as for membrane proteins. The aim is the identification of those motions that are important for the function of the protein. We will use quasi-elastic and inelastic scattering of neutrons with selectively deuterated biological samples. This is a promising method for the identification of the motions in the pico- to nano-second time scale. NMR, Infra-Red (IR) spectroscopy and Raman will be associated. These perspectives depend crucially on the obtention of selectively deuterated biological samples. This is becoming easier with the growing interest of the biologists for the dynamics- function relation, that might explain some not so well understood properties of their systems.
For soluble proteins, we will take advantage of the possible studies of coupled effects hydration water/dynamics by coherent inelastic X-ray scattering.
The systems that will be studied are soluble photosynthetic proteins (C-phycocyanin) and membrane proteins, reaction centers and light harvesting proteins, hyperthermophilic and barophilic proteins (transcarbamylase aspartate), parvalbumin, and hemoglobin.

iii)-Molecular dynamics simulations.

Computer simulations by molecular dynamics will be continued, in collaboration with A. Petrescu (Romania) and J. Smith (Heidelberg). A project about the slow dynamics in the nanosecond scale within the Physics and Chemistry of Living Objects Programme (CNRS) is being set up in collaboration with G. Kneller (Orléans).
We will always work in physiological conditions, in close collaboration with various teams of biologists.

In the field of polymers, the following activities will be developed :
Collaboration with ICS (Strasbourg) for the study of the dynamics of grafted fullerenes, with various geometries (stars, dumb-bells, ..). The dynamical structure factors will be measured by Spin Echo technique. They exhibit a minimum for a scattering vector that corresponds approximatively to the cross-over between the global translation and the internal modes. This a new topic.

Study of reinforced polymers. This is in a growth stage. It aims at mimicking reinforcement of polymers by solid mineral charges, and at studying model composite systems.
Adhesion between two polymer layers is studied by coupling mechanical measurements of the adhesion energy and interfacial profiles by neutron reflectivity and ion beam measurements. With the latter techniques, one may follow the penetration of the chains from one layer into the other one. The relation with the resistance of the interface should allow us to determine whether the interfacial chains play the role of connectors between both layers.

The experimental and theoretical studies of multiblock copolymers at interfaces will be continued. These will be made by local and outside LLB experimentalists for the studies about beta-casein. There should also be studies on synthetic copolymers manufactured by Elf-Atochem.
Studies of polymers grafted on vesicles will also be continued, in order to understand the consequences of grafting both on the structure of the polymers and of the vesicles.

INFLUENCE OF THE NEMATIC ORDER ON RHEOLOGY AND CONFORMATION OF STRETCHED COMB-LIKE LIQUID CRYSTALLINE POLYMERS.

V. Fourmaux-Demange[1], A. Brûlet[1], F. Boué[1], P. Davidson[2], P. Keller[3], L. Hilliou[4], P. Martinoty[4], J.P. Cotton[1]

[1]Laboratoire Léon Brillouin (CEA-CNRS) [2]LPS, Université Paris XI, Orsay. [3]Institut Curie, Paris. [4]LUDFC, Strasbourg

Thermotropic liquid-crystalline polymers combine the long-range orientation phases with the mechanical properties of polymers. We study **melts of comb-like liquid-crystalline polymers** in which the mesogenic part is linked as a side-chain on each unit of a flexible polymer (see Fig.1). The understanding of **the dynamics of these materials** in the nematic phase raises fundamental questions: what is the influence of the **comb-like structure?** And what is the specific effect of the **nematic interaction** on the dynamics?

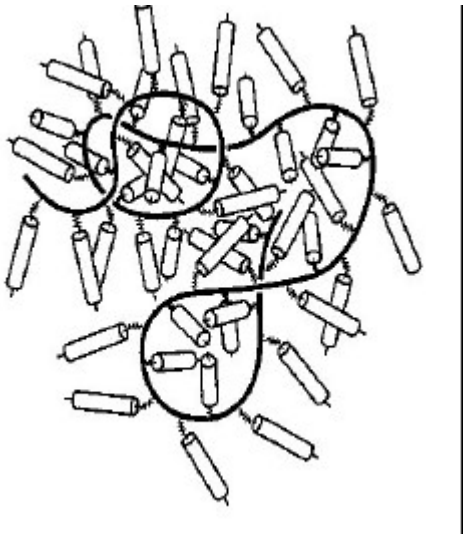

Figure 1. Schematic representation of a comb-like liquid crystalline polymer in an isotropic state.

For this purpose, we have synthesized **two isomers** of a comb-like polymetacrylate polymer (Fig.2). One polymer displays **a nematic phase** over a wide temperature range, between the glass transition temperature, T_g=44°C, and the nematic to isotropic transition temperature, T_{N-I}=83°C. Its isomeric form only has **an isotropic phase** above a glass transition temperature, T_g=32°C. The comparison of the dynamics of the nematic polymer with that of its isotropic isomer and that of the linear amorphous polystyrene allows us to dissociate the contributions due to the comb-like structure and to the nematic interaction.

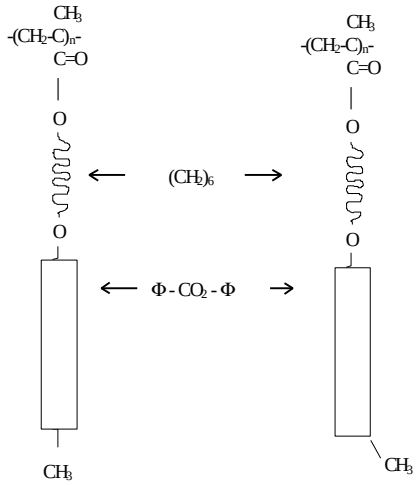

Figure 2. Chemical formula of the polymer and its isomeric form

For this study, we have associated :

- **classical rheology**, in order to obtain the characteristic times of the polymer chains both in the isotropic and nematic phases,
- **Small Angle Neutron Scattering** (SANS), in order to measure the chain conformation relaxation after an uniaxial stretching,
- **X-Ray scattering**, in order to obtain the average orientation of the mesogenic moieties in the nematic deformed samples.

Due to an important work of synthesis and fractionation of the polymers, such a study has been performed, for the first time, on polymetacrylate chains of **well-defined molecular weights.**

In the isotropic phase, our SANS study [(1)] shows that the conformation of the backbone of the comb-like polymers is similar to that of the linear polystyrene. Indeed, we have measured the variation of the radius of gyration, $R_g = 2.75N^{1/2}$, and the persistence length, $l_p \cong 10\,\text{Å}$. Thus, despite the presence of a hanging group of about 23 Å length every 2.5 Å of monomer, the **conformation of the polymetacrylate backbone is that of polystyrene**. The local rigidity due to the mesogenic group is not transmitted to the

backbone, probably because of the flexibity of the spacer $-(CH_2)_6-$.

For the dynamic study, our measurements[2] by classical rheology (a shear of small amplitude) confirm previous results[3] and show only little differences between the complex modulus curves (G', G'') in the isotropic and nematic phases. A time/temperature superposition can be established across the isotropic to nematic transition leading to unique master curves for the complex moduli (see Fig.3). The absence of a rubber plateau on these curves for polymers with degrees of polymerization N in between 40 – 1000, shows that **these comb-like polymers are not entangled**. For linear polystyrene, the average number of monomers between two neighboring entanglements is 180. Nevertheless, the observed dynamics is different from the Rouse dynamics expected for free chains. Indeed, the terminal times varies as $\tau_{ter} \propto N^{2.6}$ instead of $\tau_{ter} \propto N^2$ for a Rouse dynamics, the viscosity $\eta_0 \propto N^{1.3}$ and not $\eta_0 \propto N^1$. These results suggest a **more collective dynamics for the comb-like polymers than for linear polystyrene**.

The SANS experiments[4] allow us to describe the chain conformation of the deformed samples by two parameters: λ_p, the global chain deformation and p, the number of monomers of locally relaxed sub-chain. For a linear polymer in a Rouse regime, the chain deformation is affine (λ_p is equal to λ_s the deformation ratio of the sample) and p increases with the relaxation time t_R as $p \propto t_R^{1/2}$. For the isotropic comb-like polymer, the chain deformation λ_p remains constant, but is smaller than the sample deformation λ_s : **the chain deformation is pseudo-affine**. Meanwhile, the p values increases as $p \propto t_R$. To explain these results, we assume the existence of **living clusters** made of **temporary junctions between teeth of the comb**. The chain dynamics observed in the isotropic phase involves movements more rapid than a simple Brownian motion. If such effects probably come from specific interactions between teeth of the comb, their exact nature is still an open problem.

In the nematic phase, the chain deformation is also pseudo-affine as in the isotropic phase. But here, when the relaxation time increases, the chain deformation decreases as a stretched exponential function of the rheological terminal times (τ_{ter}) (see Fig.4). The p values are small, and remain constant; they only depend on the stretching temperature. We observe a slowing down of the chain dynamics. The **nematic interaction hindered the local relaxation of the chains**; the lifetime of the junctions is strongly prolonged. Therefore, the chain relaxation is the same at all scales.

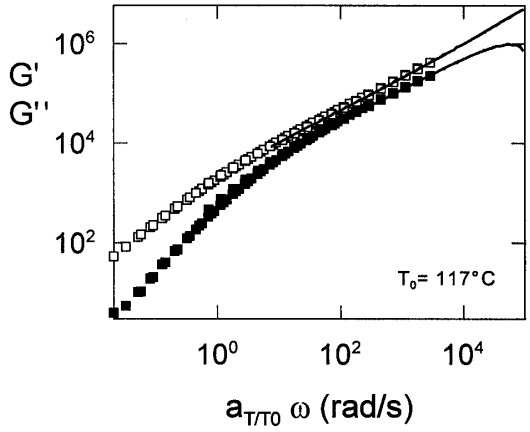

Figure 3. Master curves of the complex moduli G' G'' (unit : Pa) obtained from the time temperature superposition of the measurements obtained for the polymetacrylate polymer in the nematic phase (lines) and in the isotropic phase (G' (full symbols), G'' (open symbols). a_{T/T_0} *are the shift factors. The reference temperature* T_0 *is 117°C.*

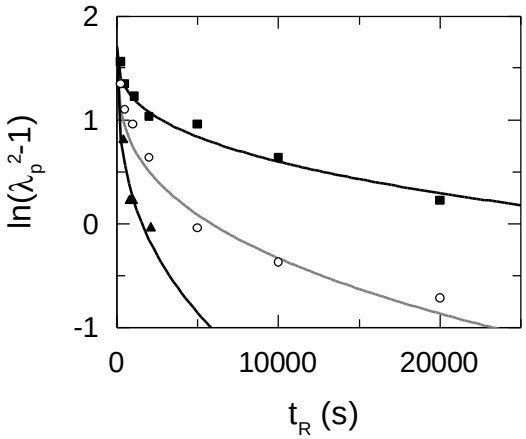

Figure 4. Relaxation of the global chain deformation of the nematic polymetacrylate of three different molecular weights. (square) M_w*=260 000 ; (o)* M_w*=130 000; (triangle)* M_w*=75 000. The full lines are the fits to a stretched exponential* $\exp[(-t/\tau_{ter})^{0.35}]$*. The exponent, 0.35, shows that the nematic interaction slows down the chain relaxation processes.*

[1] Fourmaux-Demange, V.; Boué, F., Brûlet, A., Keller, P.;. Cotton, J.P. *Macromolecules* **31** (1998) 801.

[2] Fourmaux-Demange, V.; Brûlet, A.; Cotton, J.P.; Hilliou, L.; Martinoty, P.; Keller, P.; Boué, F. *Macromolecules* **31** (1998) 7445.

[3] Colby, R.H.; Gillmor, J.R.; Galli, G.; Laus, M.; Ober, C.K.; Hall, E. *Liq. Cryst*., 13 (1996) 233

[4] Fourmaux Demange V., Thèse, University Orsay.1998.

RELATION BETWEEN THE PROFILE AND THE MECHANICAL STRENGTH OF AN INTERFACE BETWEEN TWO POLYMERS.

G. Bacri[1], M. Geoghegan[2], A. Menelle[1], C. Creton[3], F. Abel[4], F. Boué[1]

[1]Laboratoire Léon Brillouin, CEA Saclay, 91191 Gif/Yvette
[2]Lehrstuhl für Physikalische Chemie II, Universität Bayreuth, D-95440 Bayreuth
[3]Laboratoire PCSM, ESPCI, 10 rue Vauquelin, 75231 Paris Cedex 05
[4]Groupe de Physique des Solides, UMR 75 88, 2 place Jussieu 75251 Paris Cedex 05

The understanding of the mechanical resistance of an interface between two polymers is very important for the control of adhesion, fracture and interfaces/ interphases in composites polymer systems. Industrial applications are numerous. Here we focus on elastomers, which are often present in these systems. We are interested in the relation between :

- the profile of an interface created between two polymer layers. If one layer is made of perdeuterated polymer, and the second of non-perdeuterated polymer, neutron reflectivity gives access to this profile on the 10 Å to 100 Å scale ;
- and the mechanical strength of such an interface, measured using the razor blade test (from 2 to 300 J/m^2).

We have considered the three cases where none of the layers, one or both are cross-linked. The chains are always polystyrene. In the absence of cross-linking, we have a polymer melt, which is liquid above the glass transition Tg.=100°C. With cross-linking we have a statistical network, where the cross-links are distributed at random. We characterize it by the average number of units between two successive cross-links, **N**, obtained from chemical titration.

Making the sample (Figure 1).
The samples for the two methods have been done in order to get interfaces as similar as possible.

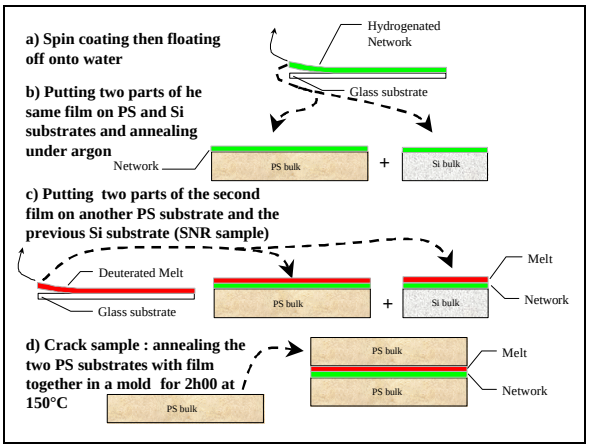

Figure 1. Making the sample

The layers, with thickness of several thousands Å, are made by spin coating on glass a polystyrene solution, or from aminomethylated polystyrene, which is chemically cross-linked during and after the drying process (Figure 1a). Each layer is removed from the glass by immersion into water (floating). We divide it in two halves (Figure 1b).
For neutron reflectivity, one deuterated half is deposited onto a Silicon wafer, annealed, then a non perdeuterated half is floated on top (Figure 1c). The sample can be annealed for a time t_R.
For the razor blade test, each of the two halves is floated on a thick polystyrene plate (2mm). After a first annealing, the plates are pressed against each other in order to form a 4-fold sandwich, during a time t_R (Figure 1d).
In both cases the interface can be studied as a function of the annealing time t_R.

Neutron reflectivity data (Figure 2)
They are obtained on the time-of-flight spectrometer EROS of LLB, for two angles θ (1.3° and 1.5°) with wavelengths in the range 4 Å to 25 Å. We take advantage of the difference in effective index between perdeuterated and non perdeuterated polymers. We have simulated the reflectivity by a profile of concentration in deuterated polymer, which is close to symmetric, by the error function from the classical laws of inter-diffusion. We give in Figure 2 the equilibrium widths σ, when the profile does not spread anymore with increasing annealing time, for the diffusion of polystyrene chains into a polystyrene network for N around 250.
In a first regime of low molecular weight M, the chains diffuse inside the network by more than their own size: $\sigma > R_g$. In the corresponding intermediate stages, we can measure the diffusion coefficients directly from the widening of the interface with time. We observe that the chains are noticeably slower than in a melt.
In a second regime of larger molecular weight, σ is lower than the global size of the chain ($\sigma < R_g$). The large chains do not penetrate completely because their entropy of mixing becomes too low to balance the elastic deformation energy due to their presence in the network. The limit size of the interface is close to that of a polymer strand between two cross-links (i.e. a piece of chain of N units).
Thus, by varying N or the molecular weight, we have the possibility of tuning at will the interfacial width, and to see its effect on adhesion between the layers.

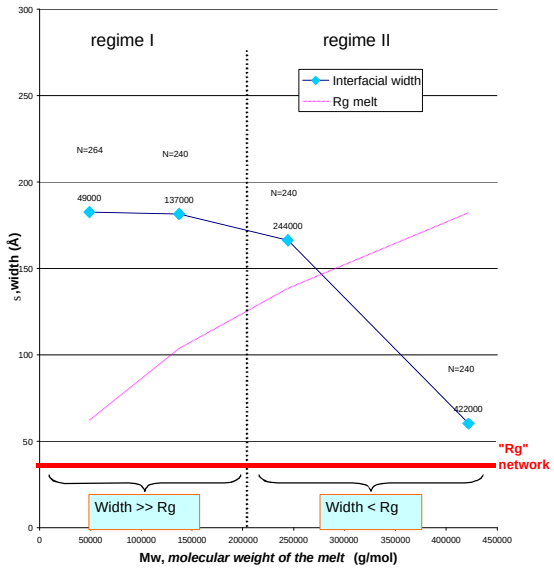

Figure 2. Neutron reflectivity data showing variation of the interfacial width s versus the molecular weight of the melt, M_w.

Razor blade test data (Figure 3, 4, 5).
In order to measure the adhesion energy, we insert a razor blade in the symmetry plane of the 4 fold sandwich, between the two polymer layers (Figure 3). The thick plates are here to store some elastic energy of bending, which will transfer into a plastic zone of deformation at the tip of the fracture. The distance **a** between the blade and the tip (measured after waiting 24 hours) gives the surface energy **G (J/m^2).**

Figure 3. Razor blade test

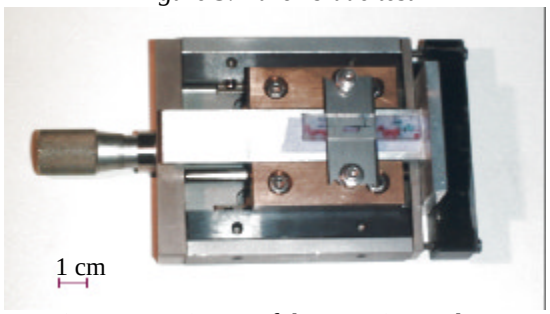

Figure 3a : picture of the experimental test

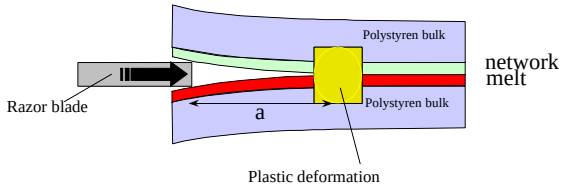

Figure 3b : diagram of test

After that the fracture has completely propagated, we can control by ion beam tests the amount of deuterium on both sides of the fracture. Thus we can check whether the fracture propagates between the perdeuterated and non-perdeuterated layers. We have also made microscopy observations of the tip zone (Figure 4**)**: the usual propagation is by a stick slip process: one has deviation with respect to the symmetry plane (an asymmetric mode called 2), until a new fracture restarts in the symmetry plane. One can also observe interference fringes ahead of the tip, in the craze region (polymer-specific cracks made of fibrils of chains).

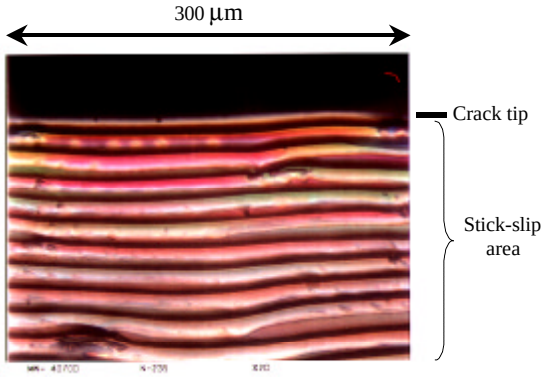

Figure 4. Top view of a crack sample made of a melt (Mw= 40700 g/mol) and a network (N=235 units between cross-links).

Figure 5 shows that in the molecular weight range I of Figure 2, the toughness **G** increases. This could be explained by the increasing degree of entanglement of a longer chain inside the network (indeed it is observed for two uncross-linked layers that **G** increases with s). Conversely, in regime II (R_g>σ), this effect should stop since the width s stops increasing. However, we see in Figure 5 that **G** keeps increasing. As an explanation, we only see at the moment the viscoelastic dissipation, which increases with molecular weight, or a kind of "knotting" of the long chains at the interface (see below).

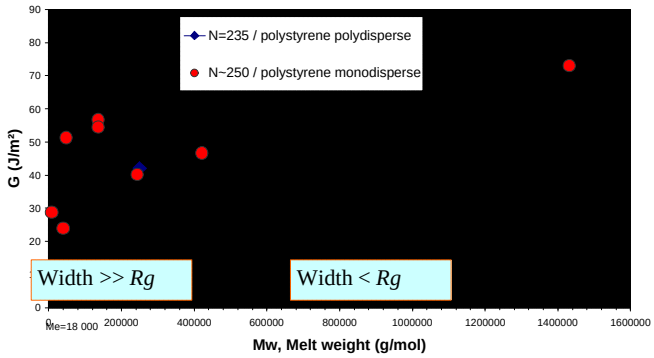

Figure 5. Plot of the toughness of the interface versus the molecular weight of the melt, M_w, static measurements

In summary, we are able to vary the interfacial width in some equilibrium conditions, which gives us a way to observe the influence of this width on the interfacial strength. It seems that the width is not the only driving parameter. Another one could be the configuration of the chains at the interface: a simplistic idea is the formation of loops by long chains in and back out of the network. We plan now to use different degrees of cross-linking in order to vary this configuration.

INTERACTION OF A THERMOSENSITIVE POLYMER WITH SURFACTANT AT THE AIR-WATER INTERFACE

B. Jean[1], L.T. Lee[1], B. Cabane[2]

[1]Laboratoire Léon Brillouin (CEA-CNRS)
[2]PMMH, ESPCI, Paris

The ability to trigger a strong response with a low-level stimulus is one of the remarkable features in soft condensed matter. In colloidal systems, these responses may be expansion or collapse of a macromolecule, dispersion or self-assembly of small molecules and specific binding or unbinding between two components. The common external parameters that can generate these transitions in behavior are temperature, solvent quality, pH, specific ions and the action of a force field. For instance, there is a family of polymers which is soluble in water at low temperatures but phase-separates out of water when heated above a critical temperature, T_c. A particularly interesting example of this family of thermosensitive polymers is poly(N-isopropylacrylamide) (PNIPAM), that has an expansion-collapse "switching" temperature at 33 °C, near the body temperature. This makes it biologically important, with potential applications[1] which include immunoassay technology and enzyme isolation where a two-phase partitioning technique is used to separate antigens and enzymes. Another important application which involves the coil-globule collapse is rate-controlled drug release. As a general viscosity modifier, its thermosensitivity provides an additional controlling parameter compared to other polymers.

Our interests lie in the applications of PNIPAM to systems that contain interfaces, such as emulsions, foams and dispersions, where the interfaces are frequently stabilized by adsorbed polymer layers. In such systems, surfactants are usually present. Therefore a relevant question is how the adsorbed polymer may be modified by other surface-active molecules. In this case, changes may occur directly at the interface where the polymer and surfactant may compete for adsorption sites or, they may mutually enhance their adsorption. Alternatively, changes may arise from interactions of the two species in the bulk phase, modifying the chemical potential of the adsorbing species and the equilibrium between the bulk and the surface. Indeed, it has been shown that PNIPAM interacts very strongly with an anionic surfactant, sodium dodecyl sulfate (SDS) in solution, resulting in a shift in the T_c to higher temperatures[2].

In this work, we investigate the effects of such interactions at the air-water interface. There are two main points of interest: firstly, how will PNIPAM adsorption be affected by the presence of SDS? Secondly, are their interactions and their resulting structural properties in solution reflected by those at the interface? To address these questions, we have used neutron reflectivity to determine the properties of the adsorbed polymer layers. Neutron reflectivity, coupled with isotopic substitution where the index of refraction of a component can be adjusted to match that of the solvent, is the only technique which allows the study of individual components in a mixed surface layer.

Figure 1 shows the sensitivity of neutron reflectivity to the presence of adsorbed PNIPAM at the air-water interface. The figure shows the normalized reflectivity, R/R_f, versus the momentum transfer, Q. R_f is the Fresnel reflectivity of the pure solvent. In this representation, any deviation from $R/R_f = 1$ is due only to the adsorbed polymer layer: the larger the deviation, the higher the amount of polymer adsorbed. These reflectivity curves also show the sensitivity of PNIPAM adsorption to temperature - an increase in temperature increases adsorption, a result due to a decrease in solvent quality. The continuous lines are the best-fits to the data using the concentration profiles shown in the inset. The profile consists of a thin monomer-rich zone near the surface followed by a central diffuse zone. As temperature increases, the monomer-rich zone becomes thicker and the central zone increases in density. Only a small increase in the overall thickness of the adsorbed layer is obtained.

The effect of surfactant on the adsorption of PNIPAM was investigated using SDS whose refractive index is matched to that of the solvent, allowing only the signal from the polymer to be registered. In Figure 2, the adsorption density of PNIPAM, Γ_p, obtained by integration of the concentration profile, is shown as a function of SDS concentration, C_s. At low C_s, PNIPAM adsorption is unaffected; at high C_s, it decreases progressively until very little polymer is left at the surface. Interestingly, the surfactant concentration at which Γ_p starts to

decrease corresponds to the critical aggregation fluorescence technique (2), where the surfactant interacts with the polymer in the bulk phase. This loss of polymer from the surface is observed even at high temperatures where the steep rise in adsorption is attenuated and pushed to higher temperatures (Figure 3).

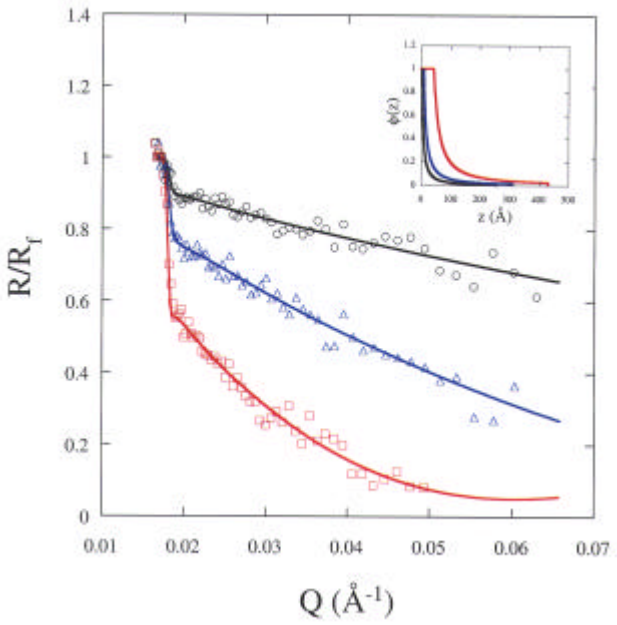

Figure 1. Normalized reflectivity of PNIPAM (M_w = 165 K) adsorbed at the air-water interface at T=20.2 °C (black circles), T=28.2 °C (blue triangles) and T=31.2 °C (red squares). The solid lines are best-fit curves using the concentration profiles shown in the inset.

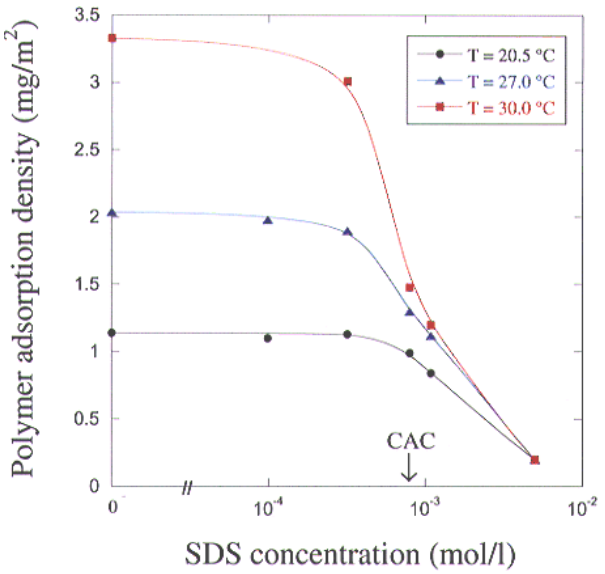

Figure 2. Effect of SDS on the adsorption density of PNIPAM.

Two possible reasons can account for the loss of polymer from the surface: it is displaced by an increasing surfactant pressure, or, it is depleted from the surface due to complexation with surfactants in the bulk solution. However, surface tension results show that in the range of C_s where the polymer is displaced, the surface pressure of the polymer layer is greater than that of the SDS. This fact strongly suggests that the loss of polymer from the surface is related to polymer-surfactant complexation in the bulk. Such complexes have been studied using small angle neutron scattering[3]. It is found that above the CAC, the mixed aggregate has a "necklace" structure consisting of several micellar aggregates adsorbed on a polymer chain (Figure 4). Above T_c, the phase-separated PNIPAM is resolubilized by SDS in two steps: at low C_s, the precipitated polymer is dispersed into colloidal particles, and at high C_s, these particles are solubilized into charged "necklaces".

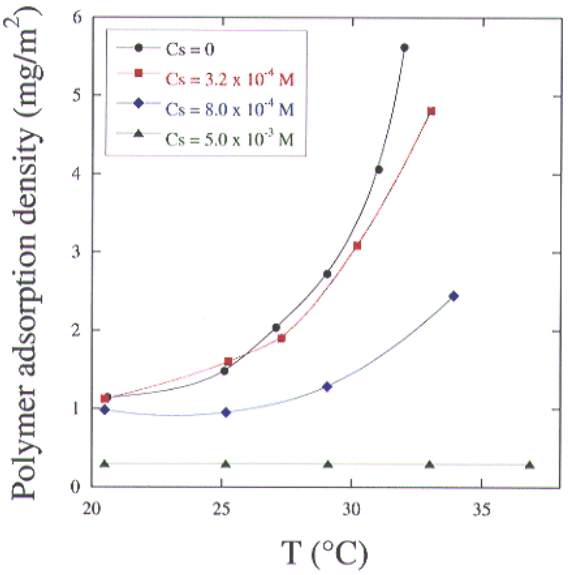

Figure 3. Effect of temperature on the adsorption density of PNIPAM in the presence of SDS.

At the surface, the loss of polymer above the CAC can therefore be attributed to the formation of charged polymer-surfactant "necklaces" in the bulk phase. In this case, what is the structure of the polymer that is left at the surface? Is the charged "necklace" structure observed in the bulk conserved at the surface? The concentration profiles in Figure 5 show that in the absence of surfactant, an increase in temperature produces a dense adsorbed layer due to reduced excluded-volume interactions between monomers. At the same temperature in the presence of SDS, a diffuse layer is obtained. This result suggests strongly the presence of micellar aggregates, the repulsions of which decrease the monomer

packing density in the adsorbed layer even at raised temperature (Figure 6).

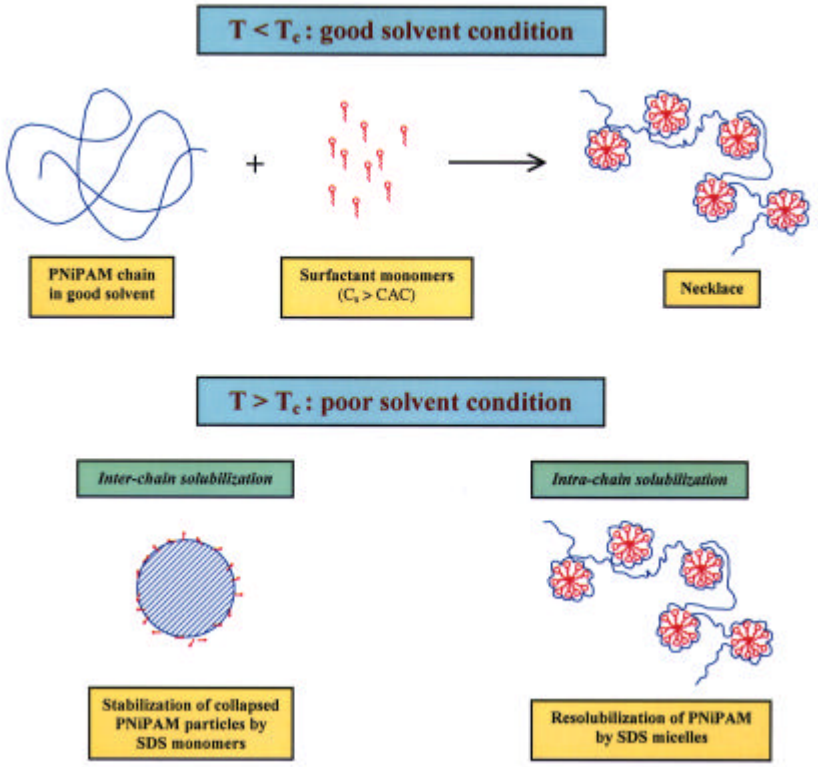

Figure 4. Interaction of PNIPAM with SDS in solution below and above the critical temperature T_c.

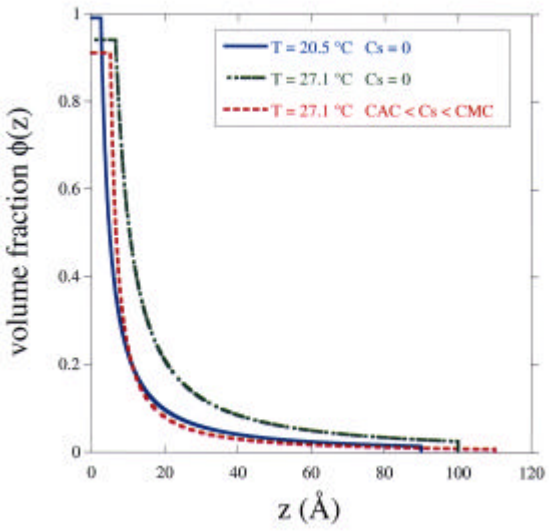

Figure 5. Concentration profiles of adsorbed PNIPAM: effects of temperature and surfactant (CMC = Critical Micelle Concentration).

In summary, PNIPAM adsorption at the air-water interface is very sensitive to small variations in temperature. In the presence of SDS, the polymer is progressively displaced from the surface due to formation of charged polymer-micelle "necklaces" in solution. Furthermore, the sensitivity of the polymer adsorption to temperature is attenuated and pushed to higher temperatures. This behavior parallels the solubilization of PNIPAM by SDS in the bulk phase and the resulting elevation in T_c. Therefore, PNIPAM-SDS interaction at the surface reflects that in the bulk solution. The concentration profiles of the adsorbed polymer show that diffuse or dense layers can be obtained, depending on the temperature and surfactant concentrations. Therefore, it is possible to modulate the T_c of PNIPAM by addition of SDS, and to control the molecular structures of the polymer both in solution and at the surface: swollen coil or collapsed globule in solution, and diffuse or dense adsorbed layers at the interface. This permits a great flexibility in tailoring the transition of the molecular structures of the thermosensitive polymer to specific uses both in solution and at interfaces.

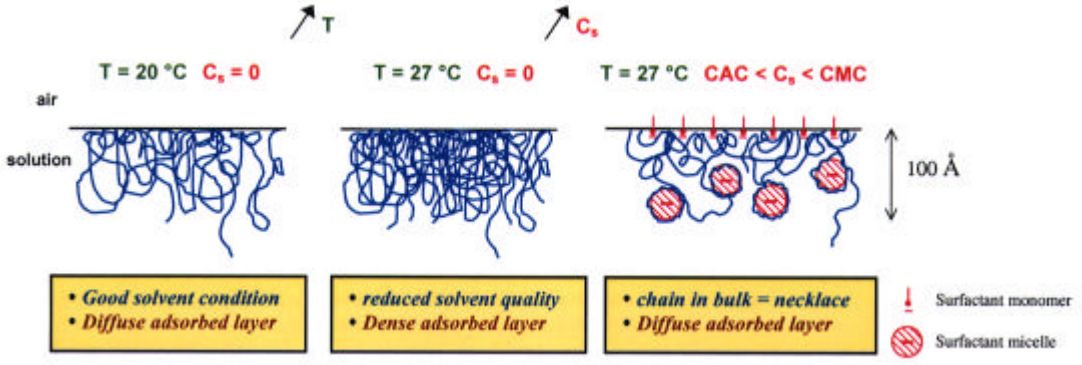

Figure 6. Structure of adsorbed layer of PNIPAM at the air-water interface: effects of temperature and surfactant.

References

[1] H.G. Schild, Prog. Polym. Sci. **17** (1992) 163.
[2] H.G. Schild and D.A. Tirrell, Langmuir **7** (1991) 665.
[3] L.T. Lee and B. Cabane, Macromolecules **30** (1997) 6559.

STRUCTURE FUNCTIONS OF STAR-BRANCHED POLYELECTROLYTES

M. Heinrich, M. Rawiso, J.G. Zilliox

Institut Charles Sadron, CNRS-ULP, 6 rue Boussingault, 67087 Strasbourg cedex

Unusual structure functions have been measured for salt-free aqueous solutions of sodium sulfonated polystyrene (NaPSS) star-branched polyelectrolytes. Whatever the concentration, they display two kinds of maxima (figure 1). The first is related to a position order between star cores. It covers a main maximum at q_1^* and a further harmonic at $\sqrt{3}\,q_1^*$ for the lower concentrations in the dilute regime. The second comes into sight at higher q values. It involves one maximum at q_2^*, quite similar to the broad halo observed in the scattering pattern of a semidilute aqueous solution of NaPSS linear polyelectrolytes. It is therefore associated with a correlation hole of electrostatic character.

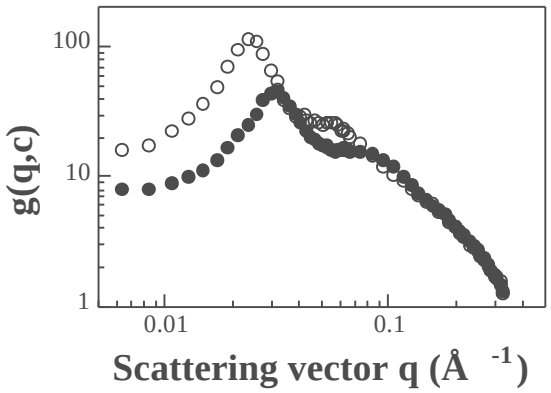

Figure 1 : Structure functions of NaPSS star solutions obtained on the spectrometer PACE at LLB
The NaPSS star sample corresponds to f=12, N_a=100 and t_S=1. Two concentrations are considered : c=0.102 mol.l^{-1} (open circles) ; 0.258 mol.l^{-1} (dark circles)

The variations of q_1^* and q_2^* with the monomer concentration c allow to stress the difference in nature of these maxima (Figure 2).
q_1^* almost scales as $c^{1/3}$ with prefactors depending on the star functionality f and the arm degree of polymerization N_a. No dependence upon the arm degree of sulfonation τ_S, has been found in the τ_S-range providing solubility of the NaPSS stars. Obviously, such results support the close relation between q_1^* and the mean distance between star cores ($d = 2\pi/q_1^*$), i.e. the short or long range order character of the first maximum.

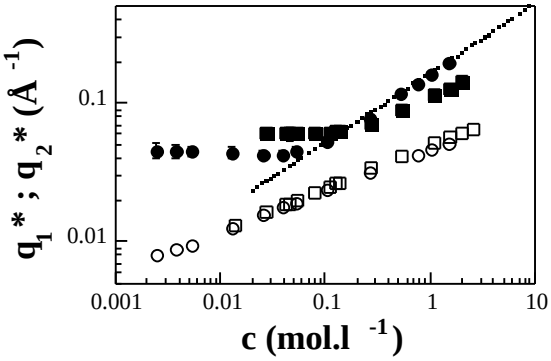

***Figure 2** : Scattering vectors q_1^* and q_2^* associated with the main maxima of the NaPSS star structure functions*
Two NaPSS star samples are considered. They have the same functionality (f=12) and arm degree of polymerization (N_a =100), but distinct t_S values. Open circles and squares correspond to q_1^* values measured for t_S=1 and 0.65, respectively. Dark circles and squares correspond to q_2^* values measured for t_S=1 and 0.65, respectively. The scaling law related to the electrostatic peak of NaPSS linear polyelectrolytes in semidilute aqueous solutions is also reported for t_S=1 (dotted line)

The c-dependence of q_2^* is quite different (q_1^* and q_2^* are therefore not commensurate). In the dilute regime ($c<c^*$), q_2^* is found to be constant, only depending on N_a and τ_S. On the other hand, in the semidilute regime ($c>c^*$), q_2^* scales as c^{α} with α in between 1/3 and 1/2, according to the τ_S value. Moreover, it is unaffected by any change in N_a. Such scaling laws fit those associated with the position q^* of the broad peak characterizing the structure functions of NaPSS linear polyelectrolytes in semidilute aqueous solutions. The second maximum of the NaPSS star structure functions is therefore primarily due to the existence of a correlation hole (or tube) surrounding each polyion, from which the others are expelled by the electrostatic repulsion. For $c>c^*$, it mainly corresponds to the semidilute solution formed by the interpenetration of stars and q_2^* yields its mean mesh size ξ or the Debye-Hückel screening length κ^{-1} (isotropic model). For $c<c^*$, it still represents the

electrostatic repulsion between arms. However, in that case, it is exclusively concerned with arms belonging to the same star. It is indeed a simple intramolecular feature, as demonstrated by using the zero average contrast method. Then q_2^* yields an effective screening length κ^{-1}, through the relation $q_2^* \propto \kappa$, which gives an information about the condensation of couterions inside each star. From this point of view, it is not really surprising that q_2^* is almost constant in the dilute regime. However, the results presented in figure 2 also show that the counterion condensation inside each star increases as τ_S decreases. On the other hand, the variation of q_2^* with N_a is in agreement with the existence of an internal screening length distribution. Finally, the distinct behaviours of q_2^* in both the dilute and semidilute regimes provide a way to estimate the overlap concentration c*.

A SYNOPSIS OF NEUTRON SPECTROSCOPY OF PHOTOSYNTHETIC MEMBRANE PROTEINS.

A. Gall[1,2], S. Dellerue[1,2], B. Robert[2], M.-C. Bellissent-Funel[1]

[1]Laboratoire Léon Brillouin (CEA-CNRS)
[2]Section de Biophysique des Protéines et des Membranes and CNRS/URA 2096, CEA/DSV/Saclay, 91191 Gif-sur-Yvette

Introduction.

All cellular processes, whether in prokaryotes or eukaryotes, at some stage require proteins which may be located either in the cytosol or in membranes. As a result, many different laboratories now study the function and structure of proteins. This is mirrored in the Protein Databank (PDB) where over 8700 X-ray crystal structures of proteins have been deposited. It is currently agreed that about 30% of the total number of proteins in any organism are integrated into membranes. Unfortunately, less than 1% of all the PDB X-ray crystal structures are from membrane proteins. Therefore, any information pertaining to the function, dynamics and structure of a membrane protein is invaluable.
The aim of this project is to understand the detailed energetics of membrane protein folding, and to establish a precise relationship between the structure, function and dynamics of this class of biological macromolecule, including inter- and intra-protein interactions. Therefore, it is necessary not only to know their three-dimensional structures, but also to characterise, with the highest degree of accuracy possible, the internal motions of these proteins. Motions in proteins occur over a wide range of time scales from femtoseconds (10^{-15}s) to seconds or longer. Only a few experimental techniques permit one to study these motions. Among them, inelastic neutron scattering (INS) is capable of probing motions with characteristic times in the nanosecond (10^{-9}s) to picosecond (10^{-12}s) range. In fact neutrons interacting with molecular systems at normal temperature can exchange a significant proportion of their energy with thermal excitations and these energy changes can be readily measured by a variety of techniques. Moreover INS is a spectroscopic technique which allows to study internal motions on exactly the same time-scale that is now accessible by computer simulation.

Our membrane proteins: RC, LH1 and LH2.

We have chosen to study and compare the structural and dynamic properties of three membrane proteins involved in the primary steps of photosynthesis from purple bacteria. These proteins are called the photochemical reaction centre (RC), the core light-harvesting complex (LH1) and the peripheral light-harvesting complex (LH2). Solar energy is collected by the bacteriochlorophyll (BChl) pigments in the LH proteins and the captured excitation energy is then transferred to the RC. Subsequent electron transfer within this protein yields a chemical potential gradient across the membrane that is used to drive many cellular processes. The proteins were chosen for study because: 1) The X-ray crystal structures of the LH2[(1)] and RC[(2)] have been solved to resolutions better than 2.5 Å, and their accompanying detergent rings have been visualised using neutron diffraction experiments. 2) They are produced by the bacteria in large quantities making the biochemical purification and protein characterisation processes much easier. 3) The proteins contain BChl cofactors that serve as molecular markers which monitor protein structure and conformation. 4) Finally, they form a network of interconnecting proteins within the photosynthetic membrane (see figure 1). We can monitor the influence of inter-protein contacts on the structure-function-dynamics for each of our three proteins.

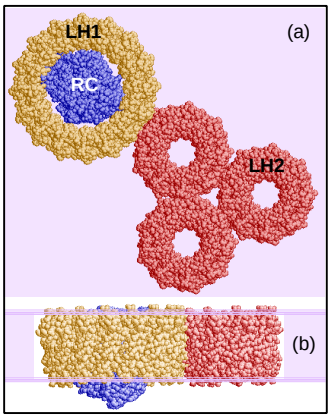

Figure 1 : A scheme of the photosynthetic integral membrane proteins from purple bacteria viewed (a) parallel and (b) perpendicular to the plane of the membrane which is coloured violet. Nearly all of the protein volumes are located within the lipid bilayer that makes up the membrane. Key to proteins : LH2, red; LH1, yellow; RC, Blue.

Principles of neutron scattering.

At this point we must remember that in INS experiment, the energy changes occurring when the incident neutrons interact with moving nuclei in the samples are measured such that an energy spectrum of scattered neutrons is obtained at each scattering angle. The fundamental quantity measured is the dynamic structure factor S(Q, ω) where Q is the momentum

transfer with $Q=(4\pi/\lambda)\sin q$ (λ is the neutron wavelength, $2q$ the scattering angle) and ω is the energy transfer. Neutron spectroscopy takes advantage of the fact that hydrogen and deuterium have different coherent and incoherent scattering cross-sections. By varying the H/D contents between the sample of interest (e.g. a membrane protein) and its environment (e.g. the membrane) we can highlight or eliminate parts of the system. This method of *contrast variation* is one reason why neutron spectroscopy may have significant advantages over similar X-ray based techniques. The benefits of neutron techniques, which may provide information on dynamics (e.g. time-of-flight and neutron spin-echo) or give structural information (e.g. small angle neutron scattering), are illustrated by presenting three examples, one from each protein, from the wide selection of experimental results obtained at the LLB (and complementary data collected at the Institute Laue-Langevin, Grenoble).

Time-of-flight spectroscopy : LH2 in detergent micelles.

A rather unique tool used to gain experimental information on protein dynamics in the picosecond range (from 0.1 to a few hundred picosecond) is incoherent inelastic neutron scattering (IINS) which takes advantage of the large incoherent scattering cross-section of hydrogen atoms with respect to the relatively small cross-section of other constitutive atoms in proteins. A large fraction of the atoms (up to 50%) in globular proteins are hydrogen atoms, and since they are distributed nearly homogeneously within the protein molecule, IINS will thus allow protein dynamics to be characterized in a global manner by monitoring the individual dynamics (vibrations, translations, rotations) of hydrogen atoms. The fundamental quantity measured is the proton self dynamic structure factor $S_S^H(Q,\omega)$.

As an example, figure 2 shows the evolution of the $S_S^H(Q,\omega)$, as a function of ω for the LH2 protein in detergent micelles. The central part is analysed as a sum of elastic and quasi-elastic components[3]. The latter component is considered to be a Lorentzian line with a half-width at half-maximum Γ. In the top left insert, Γ is plotted as a function of Q^2. It follows a plateau from 0.10 to 0.85 $Å^{-2}$ and is linearly dependent on Q^2 at higher Q^2 values. This evolution is characteristic of a diffusion in a confined volume[4] whose shape is given by the elastic incoherent structure factor (EISF) (right top insert). From the high Q limit of the EISF, it appears that LH2 contains a large proportion of mobile protons (*ca.* 90%) compared to soluble proteins such as C-phycocyanin. This may be a consequence of the rather unique hollow ring-like structure of LH2 (see figure 1). The effect of different environments on the dynamics of the hydrophobic side chains is carried out by substituting deuterated detergent by deuterated lipids.

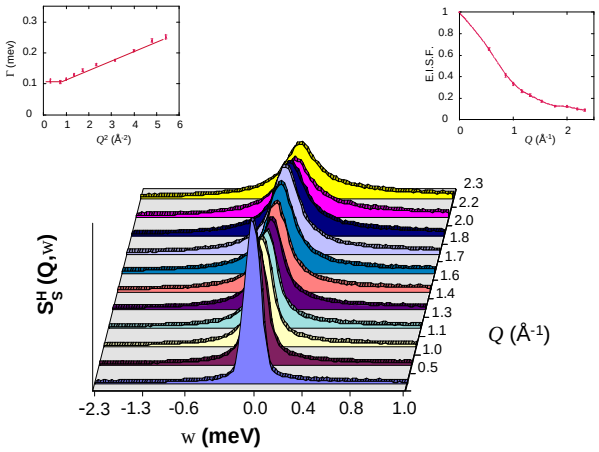

Figure 2 : $S_S^H(Q,\omega)$ of the LH2 protein in detergent micelles as a function of Q. T=277 K, l =5 Å. The spectra were collected with the time-of-flight spectrometer MIBEMOL. Top Left : Evolution of G as a function of Q^2 (see text). Top Right : Evolution of EISF as a function of Q.

Neutron spin-echo spectroscopy : Comparison between RC and LH2.

In order to study protein dynamics, *viz.* the nanosecond (10^{-9} s) time-scale, we use the neutron spin-echo [5] (NSE) spectroscopy. NSE allows precise measurement of velocity changes of neutrons via Larmor precession of the neutron's spin. If several spin-echo measurements have been made on polymers, few attempts have been made to use it to probe biological samples. Here we make use of the separation in reciprocal space of the coherent and incoherent scattering to demonstrate the detection of a neutron spin-echo signal both in RC and LH2 proteins. A further advantage of the spin-echo technique is that it gives direct access to the dynamics of the sample in the time domain t by measuring the *intermediate scattering function*, $I(Q,t)$. Figure 3 gives examples of $I(Q,t)$ for the RC and LH2 proteins for two values of Q. It is evident that the coherent motions of these complexes are somewhat different. It may be observed that at Q=0.197 $Å^{-1}$ when time, t, approaches zero, the normalised $I(Q,t)$ for LH2 is only $\approx$ 0.6 indicating that the LH2 contains significantly higher levels of sub-nanosecond motions than the RC. Although having near identical numbers of amino acids (*ca.* 850), the RC and LH2 proteins have widely differing tertiary and quaternary structures. The LH2 consists of 18 independent transmembrane spanning α-helices located within 9

identical α/β-heterodimer subunits that form a hollow ring-like structure in the membrane (see figures 1 and 3). However, the RC has three much larger subunits with less overall symmetry (blue colour in figures 1 and 3). Therefore, we conclude that the overall protein motion is dependent on the quaternary structure of the protein.

The analysis of NSE data gave us access to the effective diffusion coefficient, D_{eff} of highly concentrated protein solutions which was not possible with dynamic light scattering (DLS) experiments. By comparing the results with those of dilute solutions of proteins we have demonstrated that in the case of RC the diffuse properties are invariant over a wide range of concentrations. $I(Q,t)$ is described by an exponential function, $\exp^{(-t/\tau)}$, and $1/t=D_{eff}Q^{2}$. For our membrane proteins, DLS is limited to a maximum protein concentration of 0.8 mg ml^{-1} for which we have obtained a value of D_{eff} for the RC in detergent micelles of 3.7×10^{-8} cm^2s^{-1}. Using the spin-echo spectrometer MESS we have measured $I(Q,t)$ over Q values between 0.055 $Å^{-1}$ and 0.197 $Å^{-1}$ and have obtained a very similar diffusion coefficient of 3.6×10^{-8} cm^2s^{-1} for higher concentrations of RC in the same detergent. We are presently investigating the role of the individual domains within these proteins by selectively deuterating different components. Other approaches include insertion within lipid bilayers and, in the case of the RC, selective subunit removal.

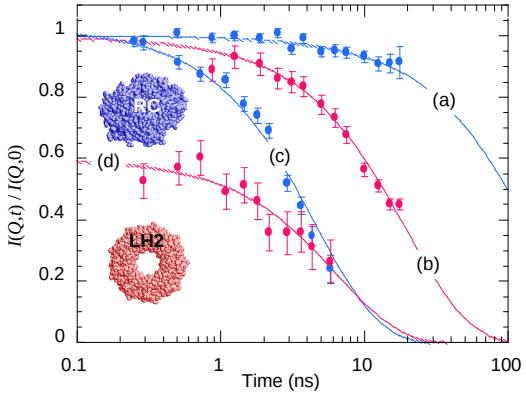

Figure 3 : The time dependence of normalised I(Q,t) for the RC (shown in blue) and LH2 (shown in red) proteins at 0.055$Å^{-1}$ (a,b) and 0.197 $Å^{-1}$ (c,d) measured at 288 K. The solid lines represent the best fits using an exponential function which may provide information on D_{eff} (see text). The spectra were collected with the spectrometer MESS. Key to proteins : LH2, red; RC, Blue.

Small angle neutron scattering : structural information on the B777 subform of LH1.

Unlike the previous two techniques which provide information on macromolecule dynamics, the *small angle neutron scattering* (SANS) technique allows us to obtain structural information. Combining SANS techniques and H/D *contrast variation* on dilute solutions, or micro-emulsions, of biological macromolecules may provide information on the shape of the molecule *via* the *form factor* and on the interactions between the molecules *via* the *structure factor*. Although we have carried out a number of different SANS experiments on the RC and LH2 proteins in different sample environments, we have chosen to present some new structural results on our third protein, LH1.

The LH1 protein is similar in overall structure and function to the LH2. However, the number of α/β-dimers increases from 9 to 16 per ring. Let us notice that this closed ring structure may only be valid for an isolated protein. *In vivo*, it is possible that the ring may be open. An important property of the LH1 protein (also called B873) is that it is possible with detergents to progressively dissociate the ring of 16 α/β-dimers into its individual α– and β-subunits (B777), *via* an intermediate form (B820). This process is shown in figure 4 and has the added advantage of being fully reversible. Since it is possible to isolate individual RC proteins, co-purify RC-LH1 complexes and the different structural units (B777 and B820) that aggregate to form LH1, one can imagine that it is possible to attribute the influence of protein-protein contacts on individual secondary and tertiary structures.

Based on biophysical data, a theory on the thermodynamics of membrane polypeptide oligomerisation in light-harvesting complexes proposed that each B777 consists of a single polypeptide sequence with a single non-covalently attached BChl molecule [6]. Recently, we decided to measure the SANS spectrum of the B777 complex in a fully deuterated detergent micro-emulsion. Figure 5 displays the data as compared with a fit using the *form factor* of an ellipsoid of length, L, of 60 Å, with a diameter, D, of 28 Å. The length of the ellipsoid is consistent with the distance required for the occupancy of a transmembrane-spanning α-helix. If the α-helix had unfolded it would not have given similar fitting parameters. Together with our Raman data [7], this is the first structural information that confirms the hypothesis that the B777 is made from one polypeptide containing a single membrane spanning α-helix with one bound BChl molecule. Further experiments with the B820 will allow to characterize the structural changes and the aggregation, that lead to the formation of the $(\alpha/\beta)_{16}$ membrane protein. This in turn will significantly help to improve our understanding of membrane protein thermodynamics and oligomerisation.

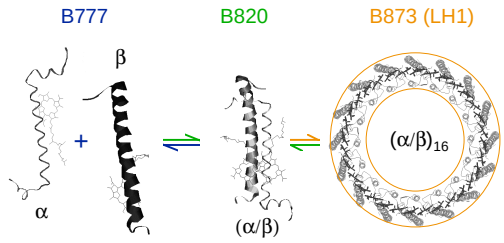

Figure 4 : The LH1 proteins are composed of a ring of 16 a/b dimers, each of which may be dissociated into individual a - and b-subunits. Each B777 polypeptide has a single non-covalently attached BChl that is responsible for capturing solar energy.

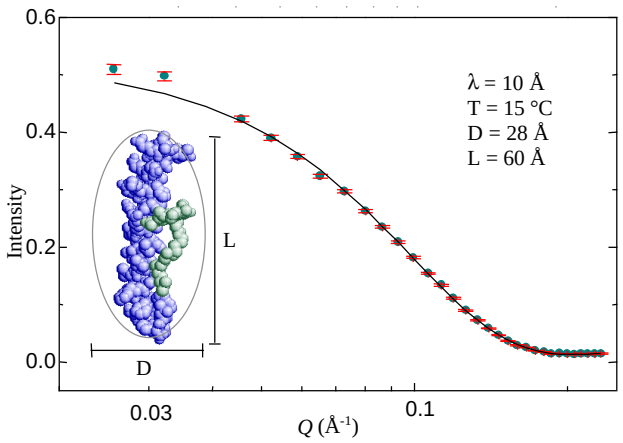

Figure 5 : SANS spectrum of the B777 complex in a deuterated detergent (D_{28}-n-octyl-ß-D-glucopyranoside) micro-emulsion. The solid line results from the fit of data with an ellipsoid (L=60 Å, D=28 Å). Therefore, each B777 subunit consists of a single protein polypeptide with a non-covalently attached BChl. The scheme of the B777 is for guidance only and is based on the X-ray crystal structure of LH2 where the polypeptide is coloured blue and the BChl blue-green. The spectra were collected with the spectrometer PAXE. T=15°C, l =10 Å.

Summary and prospectives

In summary, the photosynthetic proteins from purple bacteria provide an unique opportunity to compare the influence of tertiary structures on internal protein dynamics. Our family of interconnecting membrane proteins also allows us to measure the effect of inter-protein interaction on protein dynamics and structure. Using SANS we can obtain novel information on protein structures, as shown by our approximation of the *form factor* of the B777. Furthermore, based on experimental data from time-of-flight and NSE spectroscopies, improved pisosecond and new nanosecond molecular dynamics algorithms for membrane proteins are currently being developed.

Finally, our protein system provides an important contribution to the overall understanding of the inherent differences between integral membrane proteins and globular proteins, which are located in the cytosol. One such major physical difference is the pressure-sensitivity of proteins. In collaboration with the University of Tartu, Estonia, we have measured a series of electronic absorption and pre-resonance Fourier Transform - Raman spectra for the RC, LH1 and LH2 proteins which show that they are still intact at pressures where globular proteins, such as myoglobin, are denatured. In addition to our present series of experiments, we are presently planning Fourier Transform - Infra-Red and neutron measurements to establish the membrane protein structure-function-dynamic relationships as a function of applied hydrostatic pressure.

1. McDermott, G., Prince, S. M., Freer, A. A., Hawthornthwaite-Lawless, A. M., Papiz, M. Z., Cogdell, R. J., and Isaacs, N. W. (1995) *Nature (London) 374*, 517-21.
2. Roy, C., Lancaster, D., Ermler, U., and Michel, H. (1995) *Adv. Photosynth. 2*, 503-26.
3. Bee, M. (1988) *Quasielastic Neutron Scattering. Principles and Applications in Solid State Chemistry, Biology, and Materials Science*, Adam Hilger, Bristol, UK.
4. Volino, F., and Dianoux, A. J. (1980) *Mol. Phys. 41*, 271-9.
5. Mezei, F. (1980) *Lecture Notes in Physics, Vol. 128: Neutron Spin Echo, Springer-Verlag, Berlin.*
6. Sturgis, J. N., and Robert, B. (1994) *J. Mol. Biol. 238*, 445-54.